



Study on Influence of Local Failure of Supporting Structure on Enclosure Structure

Yaozi Wu*, Xueyan An

School of Civil Engineering, Hebei University of Engineering, Handan, China

Email: *1843013301@qq.com

How to cite this paper: Wu, Y.Z. and An, X.Y. (2023) Study on Influence of Local Failure of Supporting Structure on Enclosure Structure. *Open Access Library Journal*, 10: e10179.

<https://doi.org/10.4236/oalib.1110179>

Received: April 24, 2023

Accepted: May 22, 2023

Published: May 25, 2023

Copyright © 2023 by author(s) and Open Access Library Inc.

This work is licensed under the Creative Commons Attribution International License (CC BY 4.0).

<http://creativecommons.org/licenses/by/4.0/>



Open Access

Abstract

Foundation pit collapse is a continuous failure process. One of the main characteristics of foundation pit collapse caused by internal support failure is that it will lead to the destruction of the enclosure structure. Based on the actual foundation pit engineering, this paper uses the finite element software Midas-GTS NX to establish a three-dimensional foundation pit model. Based on the principle of component removal method and nonlinear dynamic analysis method, the influence of the inner support failure on the envelope structure is analyzed. The results show that when the damage degree of the inner support increases, the deformation of the foundation pit retaining structure also increases, and the phenomenon of stress concentration occurs. The horizontal displacement of the retaining structure increases with the increase of the local failure location, but the overall displacement has little change. With the aggravation of the local failure degree of the retaining structure, the soil deformation around the foundation pit keeps increasing, and the maximum displacement and maximum stress both increase significantly. The research of this paper can provide some safety guidance for foundation pit engineering.

Subject Areas

Civil Engineering

Keywords

Deep Foundation Pit, Partial Failure, Alternate Path Method, Numerical Modeling, Enclosure Structure

1. Introduction

Underground comprehensive pipeline corridor refers to the underground construction of a tunnel space that integrates electric power, communication, gas,

water supply and drainage, heat and other engineering pipelines, and carries out unified planning, design, construction and management. It is the “lifeline” of important infrastructure to ensure urban operation, ensure urban safety and improve the comprehensive carrying capacity of the city. In order to meet the requirements of modern city construction, it has become a trend to promote the construction of underground integrated pipeline corridors.

With the continuous development of deep foundation pit engineering of underground integrated pipe corridors, the corresponding excavation and support technology of foundation pit has been advanced and innovated to different degrees. However, the supporting structure of deep foundation pit only plays a temporary role, coupled with the existence of some uncertain factors in deep foundation pit engineering, which leads to collapse accidents from time to time, such as Yangzhou foundation pit collapse in 2019 [1], Hangzhou foundation pit collapse in 2021 [2], Singapore subway accident [3], etc. It not only caused casualties but also brought huge economic losses. According to relevant information, the collapse of foundation pit is a continuous failure process [4] [5].

For the continuous failure of engineering structures, Huang Hua *et al.* [6] made a theoretical analysis of the collapse mechanism and influencing factors, and in order to reduce the occurrence of such accidents, put forward several methods to resist collapse. Liu *et al.* [7] proposed an analytical model for the continuous failure of reinforced concrete slab column structures. Song Ge *et al.* [8] used the energy method to analyze the force characteristics at each stage of continuous collapse, and expressed the curves at each stage with expressions. Fu [9] *et al.* proposed a mechanical model for composite structures with steel frames, which is mainly used to analyze and calculate the resistance to continuous collapse of the composite structures under the condition of internal column failure. Lu [10] *et al.* proposed a better steel-concrete composite structure, which has better resistance to continuous collapse and earthquake resilience in terms of performance. Wang Junjie, Yang Tao, Yang [11] [12] [13] *et al.* have also carried out relevant studies on various combination structures, and have made their own achievements in the resistance to continuity failure.

This paper mainly uses Midas-GTS NX finite element software to establish a three-dimensional foundation pit model, and then uses the measured data and model data to verify the effectiveness. The principle of the method of removing components is adopted to simulate the local failure of the horizontal supporting structure of deep foundation pit by removing different amounts of internal supports, and then its influence on the envelope structure is analyzed [14] [15] [16].

2. Establishment of Finite Element Model

2.1. Introduction to Mdiags GTS NX

Mdiags GTS NX is a professional finite element analysis software for geotechnical engineering, featuring fast modeling, wide application and stable operation. After a large number of professional engineering practices, the feedback effect is

good, with fast convergence, good convergence of calculation results, efficient analysis results and so on. In addition, the software also contains advanced analysis kernel, which can guarantee the convergence and high efficiency of the calculation results.

Mdias GTS NX finite element software contains a large number of structural elements and sections. For complex sections, it can be realized by adding heterosexual sections, which provides convenience for 3D finite element geometric models. Grid division is fast and contains many constitutive models required for foundation pit engineering. Users can define constitutive models according to their own needs and choose analysis types according to their own analysis methods. In the output of the results of the software can also be high-definition pictures, charts and other formats, more convenient to use.

In short, Mdias GTS NX is a powerful, widely used and stable finite element analysis software, which is of great help to the comprehensive pipeline corridor deep foundation pit engineering.

2.2. Model Building

The total length of the comprehensive pipe corridor project is 951.37 m, and the standard section of the comprehensive pipe corridor is covered with about 3.0 m soil, which is constructed by open excavation method. In order to facilitate the comparison and analysis between the construction site monitoring data and the numerical simulation data, one section is selected. The excavation depth of the foundation pit of this project is 11 m and 7 m wide. According to the references, the influence range of foundation pit excavation is 3 - 4 times the excavation depth, so the geometric model size is 107 m × 85 m × 55 m. In this paper, the finite element software Midas-GTS NX is used to establish the model without considering the effect of groundwater, as shown in **Figure 1**.

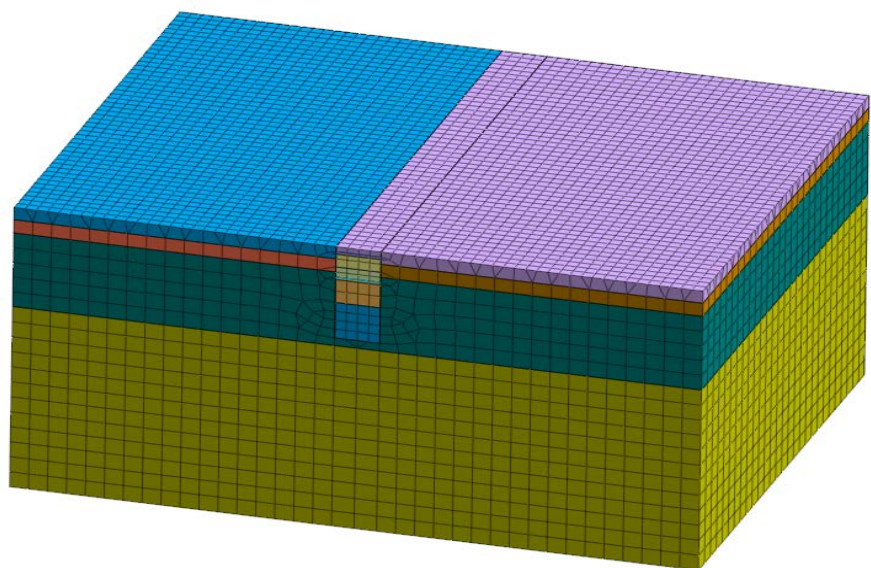


Figure 1. Foundation pit model.

According to the geological investigation report of the project, the soil layer structure is successively mixed fill, clay, silty clay with silty soil, and medium-weathered limestone. The retaining structure of the foundation pit adopts $\Phi 850@600$ SMW three-axis cement mixing pile, the pile length is 18 m, the embedment depth is 7 m, the layout type of section steel is inserted two jump one type, and it is converted into the ground connecting wall with a certain thickness according to the flexural stiffness theory [17]. The section size of crown beam is 1.2 m \times 0.8 m, and the waist beam is HN500 \times 200. The section size of the first support is 0.8 m \times 0.8 m, and the spacing is 7 m. The second inner support adopts D606 \times 13 steel pipe inner support, and the spacing is 3.5 m. The physical parameters of each material are obtained based on the geotechnical test and geological exploration report, as shown in **Table 1** and **Table 2** below.

As shown in the table above, on the premise that all components are isotropic, the soil constitutive model is selected as the modified Mol Coulomb model, and the elastic model is adopted for the ground joint wall, concrete support, steel pipe inner support, crown beam and waist beam. 2D plate element is used for the ground connecting wall, and 1D beam element is used for the inner support, crown beam and waist beam.

Table 1. Formation physical parameters.

Soil layer name	Weight/(kN·m ⁻³)	Elastic modulus/MPa	Cohesion C/KPa	Friction Angle $\phi/(^{\circ})$	Layer thickness/m	Constitutive relation
Miscellaneous fill	18.2	3.0	5	15	2.4	Modified Mole-Coulomb
Clay	17.3	4	14	6	2.6	Modified Moore-Coulomb
Silty clay with Silty soil	18.6	7.5	19	11	14.5	Modified Mole-Coulomb
Moderately weathered Limestone	24.0	5200	100	30	-	Modified Moore-Coulomb
Ground wall					0.58	

Table 2. Physical parameters of materials.

Soil layer name	Weight/(kN·m ⁻³)	Elastic modulus/MPa	Cohesion C/KPa	Friction Angle $\phi/(^{\circ})$	Layer thickness /m	Constitutive relation
Crown Beam	24	30,000			1.2 m \times 0.8 m	elastic
Concrete support	24	30,000			0.8 m \times 0.8 m	elastic
Steel pipe inner support	78.5	206,000				elastic
Section steel	78.5	206,000				elastic
Cement soil	20	700				elastic

The displacement boundary constraints in X, Y and Z directions are added to the boundary bars of the model. Add 15 KN vertical construction load and self-weight load within 10 m from the foundation pit, and the constraints can be shown in **Figure 2**. In this paper, nonlinear dynamic analysis method is used to study the mechanism.

2.3. Model Component Process

The construction conditions of this model are shown in **Table 3**. The model is mainly established according to the construction conditions in the following table.

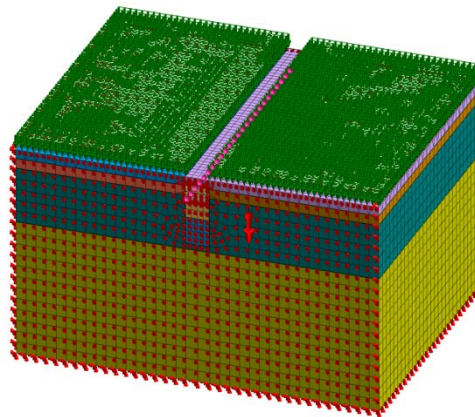


Figure 2. Model constraint diagram.

Table 3. Construction condition table.

Serial number	Content
1	Analysis of initial seepage field
2	Initial stress field equilibrium
3	Slope excavation, and shotcrete
4	Construction of enclosure structure
5	The first precipitation is 2.4 m below the ground
6	Excavate 1 to 1.9 m below the ground and erect the first inner support and crown beam
7	The second precipitation is 4.2 m below the ground
8	Excavate 2 to 3.7 m below the ground
9	Third precipitation to 6 m below ground level
10	Excavate 3 to 5.5 m below the ground and erect the second inner support and waist beam
11	Fourth precipitation 8 m below ground level
12	Excavate 4 to 7.5 m below ground level
13	The fifth precipitation to 10 m below the ground
14	Excavate 5 to the bottom of the foundation pit

2.4. Comparison between Original Model and Measured Data

The measured data in the engineering research section and the software simulation data are selected for comparative analysis, as shown in **Figure 3**. The variation trend is roughly the same and the error is within an acceptable range, so the validity of the finite element model is verified, and the software can be used to study the envelope structure.

3. Internal Support Local Failure Analysis

In the relevant data, some scholars have confirmed that the lower support is more important than the upper support, so this paper still chooses the second internal support as the research pair and will not demonstrate this. Now label the inner support in **Figure 4** for the convenience of subsequent relevant research. The finite element model of damage of 1, 3 and 5 internal supports after the completion of foundation pit excavation was established based on the principle of component removal method, that is, B2-13, B2-12 and B2-14, B2-11 and B2-15 supports were removed respectively to analyze the changes of the envelope structure [18] [19].

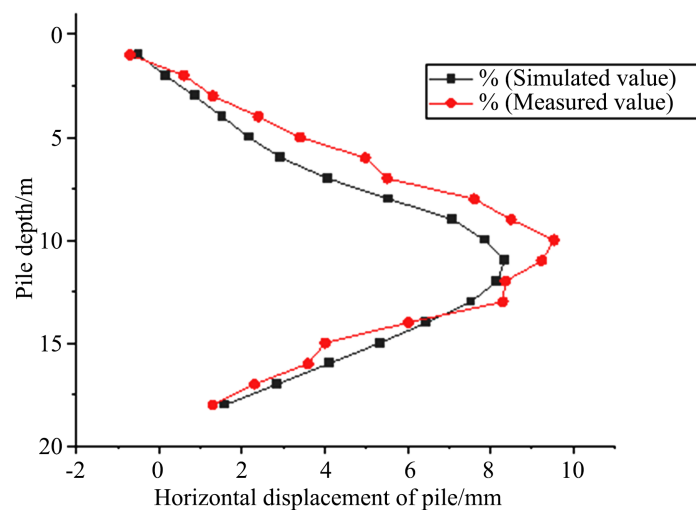


Figure 3. Comparison of simulated and measured values.

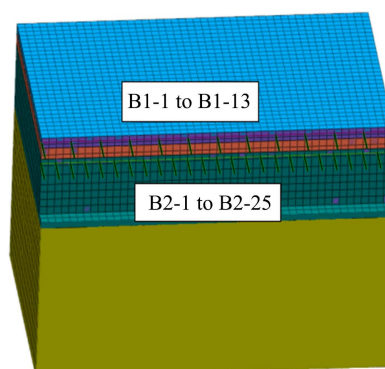


Figure 4. Schematic diagram of support numbering.

3.1. Failure of 1 Inner Support

As can be seen from **Figure 5**, when an inner support fails, the displacement of the ground connecting wall changes in a small range, mainly within the range of the inner support failure, and the influence on the side is small. In the direction along the X axis, the earth pressure of this part is relatively large due to the support failure, which has an impact on the ground connecting wall, and the maximum displacement reaches 29 mm. In contrast, the ground wall is affected by symmetry in the Y-axis direction, and its displacement is only about 0.16 mm.

As can be seen from **Figure 6**, when the internal support fails, stress concentration will occur in the ground diaphragm wall, mainly in the middle of the enclosure structure, and the maximum stress of a unit can reach 1978.97 KN/m².

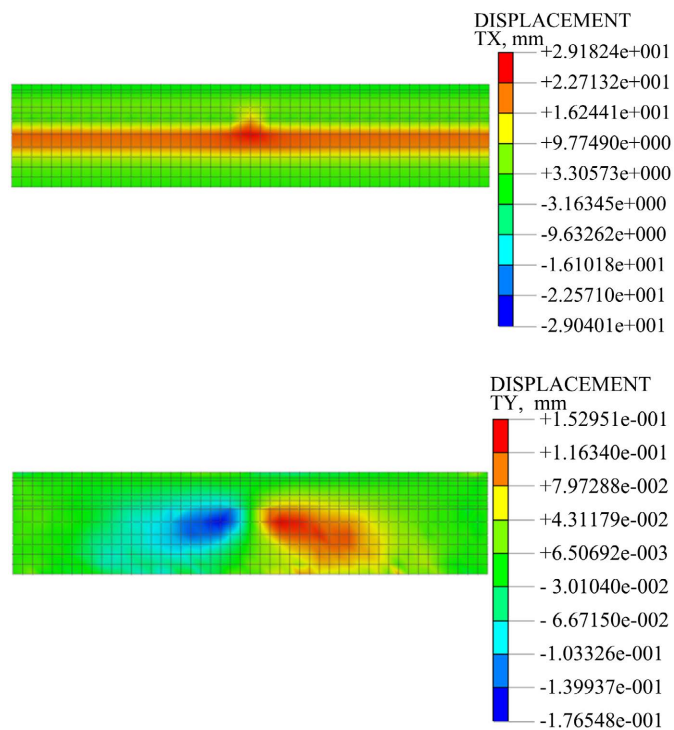


Figure 5. Cloud map of displacement change of ground diaphragm wall damaged by 1 internal support.

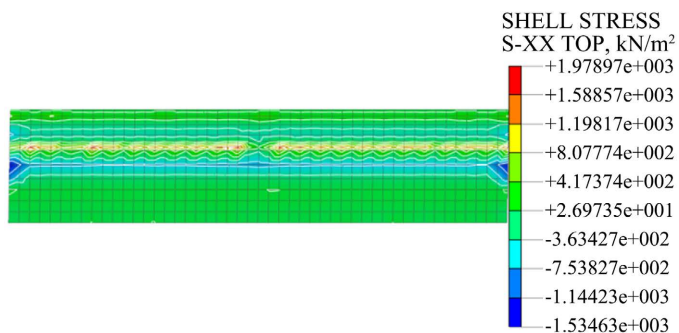


Figure 6. Stress concentration nephogram of a fractured ground wall with an internal support.

3.2. Failure of 3 Internal Supports

As can be seen from **Figure 7**, when three internal supports fail, the maximum horizontal displacement along the X-axis increases by 77 mm (2.65 times) from 29 mm (29 mm) of the failure of one root, and it can be clearly observed from the cloud map of displacement change that the affected range is also constantly expanding. At the same time, the displacement of the ground wall in the Y-axis direction is increased from 0.16 mm to 0.78 mm by 4.875 times, and the affected range is more concentrated and wider.

According to the stress concentration cloud map of the ground connecting wall in **Figure 8**, the contours on the figure clearly show that the stress concentration phenomenon is more obvious when the three internal supports fail, and the maximum stress value at one place can reach 3137.32 KN/m^2 , which increases by 1.58 times compared with the failure of one root.

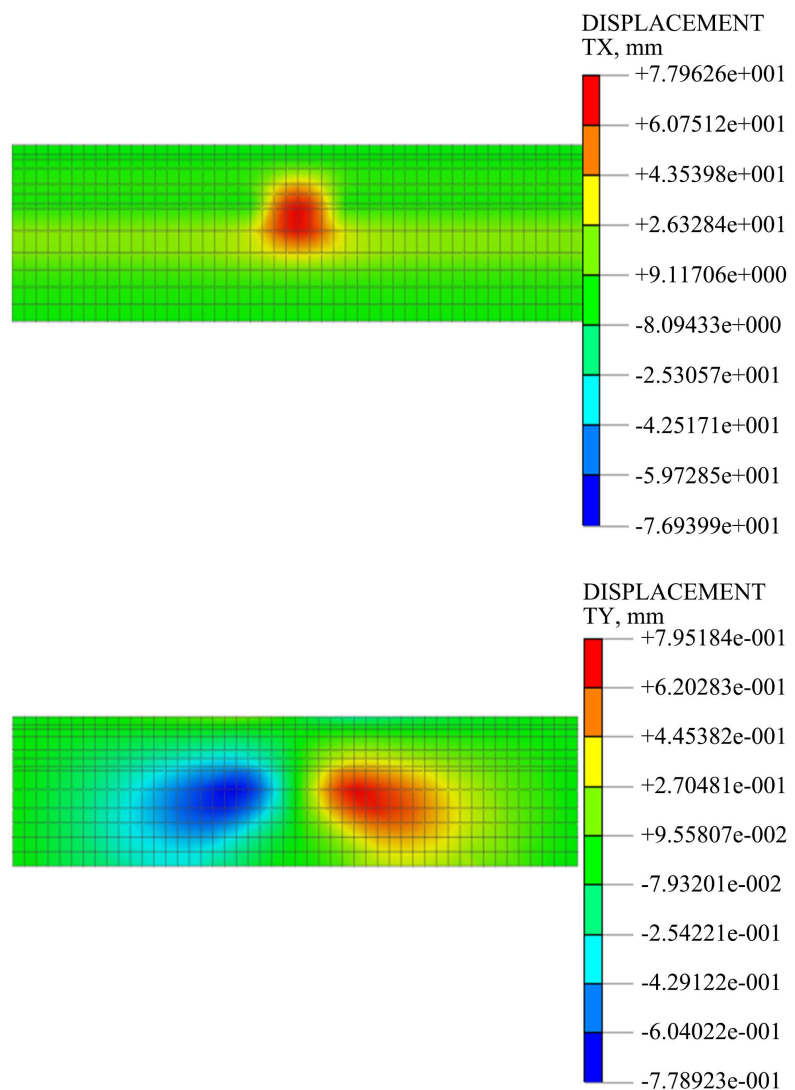


Figure 7. Cloud map of displacement change of ground wall with three internal supports damaged.

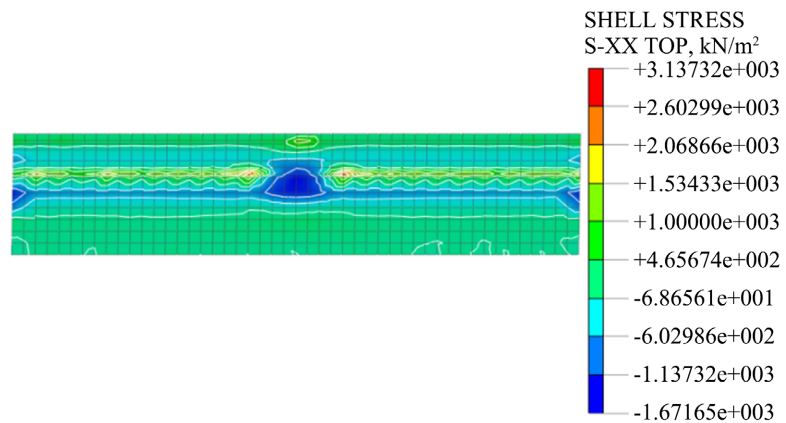


Figure 8. Stress concentration nephogram of fractured ground wall with three internal supports.

3.3. Failure of 5 Internal Supports

As can be seen from **Figure 9**, when 5 internal supports fail, the damage scope of the ground connecting wall is wider than that of 1 and 3, and the maximum horizontal displacement reaches 161 mm, which is 5.55 times and 2.09 times higher than that of 1 and 3, respectively. In comparison, along the Y-axis, the maximum displacement reaches 1.4 mm, which is 8.75 times and 1.79 times higher than the failure of 1 and 3 roots.

In **Figure 10** of the stress concentration cloud map of the ground diaphragm wall, according to the distribution of its contour lines, it can be more obviously observed that when the internal support fails, the phenomenon of stress is more concentrated, and the maximum stress value reaches 3939 KN/m².

Figure 11 respectively shows the horizontal difference displacement curves at the same position as the original model when the internal support fails. As can be seen from **Figure 11**, the maximum difference horizontal displacement here occurs at a depth of 7 m. Study the transverse influence range of ground diaphragm wall when support failure occurs in different quantities at a depth of 7 m: When an internal support was damaged, the transverse distance from the depth of 7 m to the observation point was 1 m, 3 m and 5 m, and the difference horizontal displacements were 1.30 mm, 0.69 mm and 0.17 mm, respectively. The displacement values of the original model were 3.40 mm, 3.10 mm and 3.57 mm, respectively, increasing by 38.24%, 22.26% and 4.76%, respectively. If an increase of more than 5% is taken as the main influence area of local internal support failure, the main transverse influence range of local failure of 1 internal support is 1.5 times of the second internal support distance on both sides of B2-13, and the transverse influence range of 3 and 5 internal supports is 3.1 times and 4 times of the second internal support distance on both sides of B2-13, respectively.

The analysis shows that with the increase of the number of removed internal supports, the horizontal displacement of pile at the same depth also increases to varying degrees while the influence range increases. At the bottom of pile, the

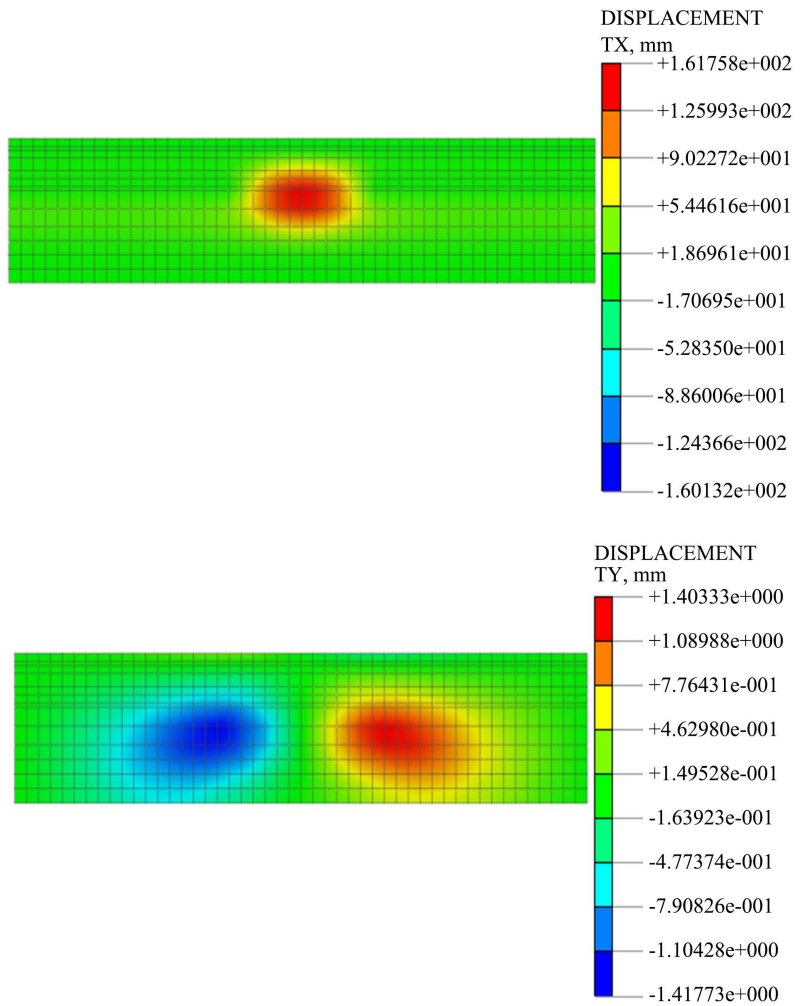


Figure 9. Cloud map of displacement change of ground connecting wall damaged by 5 internal supports.

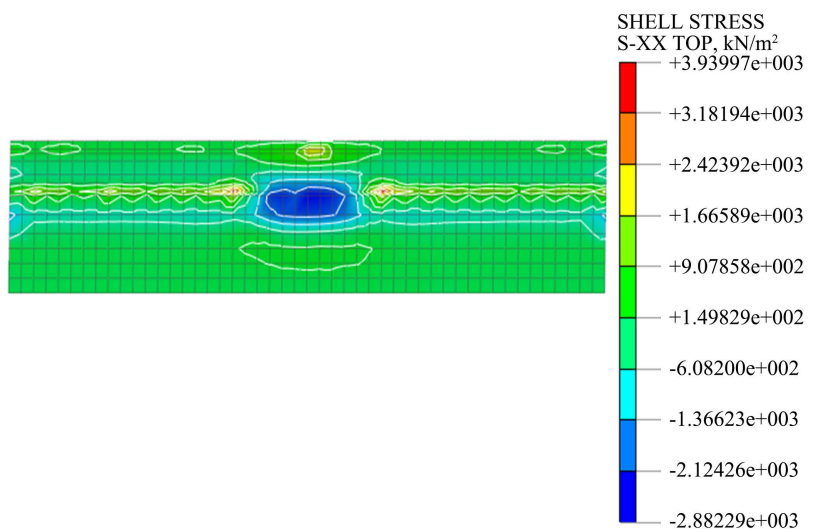


Figure 10. Stress concentration nephogram of ground diaphragm wall damaged by 5 internal supports.

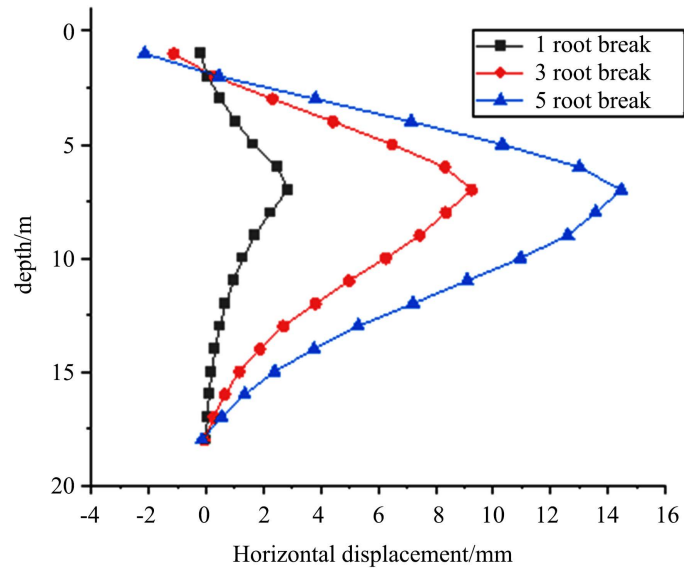


Figure 11. Horizontal displacement curve of ground connection wall difference.

degree of influence is almost negligible. Near the pile top, the opposite effect is weaker. This corresponds to that the lower support is more important than the upper support of the foundation pit supporting structure.

4. Conclusions

In this paper, Midas-GTS NX finite element software is used to establish a three-dimensional foundation pit model, through the simulation of internal support failure, to explore the impact of the envelope structure.

1) With the local failure of the supporting structure, the deformation of the foundation pit increases and the displacement develops to the pit; with the aggravation of the local failure degree of the supporting structure, the maximum deformation value of the foundation pit retaining structure increases continuously, and the phenomenon of large displacement and stress concentration appears.

2) Local failure will cause the increase in deformation and internal force of the foundation pit retaining structure. The horizontal displacement of the retaining structure increases with the increase of the local failure position, but the overall displacement changes little, which is consistent with the actual situation of the project.

3) With the aggravation of the local failure degree of the enclosure structure, a large plastic strain and stress concentration phenomenon occurs in the enclosure structure of the foundation pit; with the aggravation of the local failure degree of the enclosure structure, the soil deformation around the foundation pit increases continuously, and the maximum displacement and maximum stress increase significantly.

4) The failure of internal support has a weak influence on pile top and pile body.

When the internal support is partially damaged, the stress change law and displacement change law are obtained by analyzing the influence of the maintenance structure, which provides the corresponding basis for the needs of practical engineering.

Acknowledgements

Upon the completion of the thesis, we would like to take this opportunity to express our sincere gratitude to our supervisor, Professor Lu Lanping, who has given us important guidance on the thesis. Without her help and encouragement, our thesis would have been impossible. Besides her help with our thesis, she has also given us much advice on the methods of doing research, which is of great value to our future academic life.

We are also obliged to other teachers whose lectures have broadened our scope of vision.

Last but not least, we would like to express our gratitude to all the friends and family members who have offered us help. Without their help, we could not have finished our study and this thesis.

Conflicts of Interest

The authors declare no conflicts of interest.

References

- [1] Qi, H.W., Zhang, H.F. and Tian, B. (2018) Research on Virtual Simulation System of Major Foundation Pit Collapse. *China Work Safety Science and Technology*, **14**, 174-179.
- [2] Xiao, X.C., Yuan, J.R. and Zhu, Y.F. (2009) Accident Cause Analysis of C824 Section of Singapore Metro Circle Line (I)—The Overall Situation of the Project and the Accident Process. *Modern Tunnel Technology*, **46**, 66-72.
- [3] Mohamed, O.A. (2006) Progressive Collapse of Structures: Annotated Bibliography and Comparison of Codes and Standards. *Journal of Performance of Constructed Facilities*, **20**, 418-425. [https://doi.org/10.1061/\(ASCE\)0887-3828\(2006\)20:4\(418\)](https://doi.org/10.1061/(ASCE)0887-3828(2006)20:4(418))
- [4] Jia, J.G., Xu, Y., Shi, L. and Jin, F.N. (2008) Discussion on the Definition of “Continuous Collapse”. *Blasting*, No. 1, 22-24.
- [5] Huang, H., Liu, X.X., Huang, M. and Guo, M.X. (2022) Research Status of Continuous Collapse Failure and Performance Improvement of Engineering Structures. *Journal of Building Science and Engineering*, **39**, 29-44.
- [6] Liu, J.R., *et al.* (2015) Resistance of Flat-Plate Buildings against Progressive Collapse. I: Modeling of Slab-Column Connections. *Journal of Structural Engineering*, **141**, Article ID: 04015053. [https://doi.org/10.1061/\(ASCE\)ST.1943-541X.0001294](https://doi.org/10.1061/(ASCE)ST.1943-541X.0001294)
- [7] Song, G. and Wang, L. (2016) Resistance Analysis of Composite Beams under Collapse Condition Based on Energy Method. *Mechanics in Mechanics and Practice*, **38**, 424-431.
- [8] Qiu, N.F., *et al.* (2018) A Mechanical Model of Composite Floor Systems under an Internal Column Removal Scenario. *Engineering Structures*, **175**, 50-62. <https://doi.org/10.1016/j.engstruct.2018.07.095>

- [9] Lu, X.Z., *et al.* (2019) Improvement to Composite Frame Systems for Seismic and Progressive Collapse Resistance. *Engineering Structures*, **186**, 227-242. <https://doi.org/10.1016/j.engstruct.2019.02.006>
- [10] Wang, J.J., Wang, W. and Sun, X. (2017) Continuous Collapse Resistance Test of Column Structure in Composite Beams with Molded Steel Plates. *Engineering Mechanics*, **34**, 149-153+178.
- [11] Yang, T., Zhao, K. and Peng, X.-N. (2020) Experimental Study on Dynamic Collapse Behavior of Steel-Concrete Composite Frame Substructures. *Journal of Vibration and Shock*, **39**, 36-42.
- [12] Yang, B., *et al.* (2018) Component Tests and Numerical Simulations of Composite Floor Systems under Progressive Collapse. *Journal of Constructional Steel Research*, **151**, 25-40. <https://doi.org/10.1016/j.jcsr.2018.09.008>
- [13] Li, T., Yang, Y.W., Zhou, Y.Q., Liu, B., Zheng, Q. and Zheng, Y.X. (2022) Calculation Method of Horizontal Displacement of Support Structure in Deep Foundation Pit When Support Is Removed. *Chinese Journal of Rock Mechanics and Engineering*, **41**, 3021-3032.
- [14] Yuan, X.F. (2019) Study on Local Failure and Redundancy of Braced Pile Row Supporting Structure in Deep Foundation Pit. Chongqing University, Chongqing.
- [15] Zou, Q. (2012) Research on Foundation Pit Support Design Considering Redundancy]. Tianjin University, Tianjin.
- [16] Yu, D.Y. (2019) Research on Continuous Failure Mechanism and Control Measures of Internal Support Foundation Pit Supporting System. Tianjin University, Tianjin.
- [17] Wei, S. (2020) Study on Water Stopping Effect and Excavation Deformation of Hard Occlusal Bored Pile in Deep Foundation Pit. Beijing Jiaotong University, Beijing.
- [18] Song, L.W. and Tan, Y.Q. (2019) Research on Deep Foundation Pit Support System Based on Redundancy under Construction Conditions. *Chinese Journal of Underground Space and Engineering*, **15**, 321-326.
- [19] Gu, J.C. and Xia, J.Z. (2019) Research on Continuous Failure Mechanism of Foundation Pit of Internal Support System. *Bulletin of Science and Technology*, **35**, 75-81.